Towards a unified mechanical model for design and assessment of structural concrete members under shear, flexure and punching

Marí, Antonio[1]; Cladera, Antoni[2]; Bairán, Jesús[3]; Oller, Eva[4]

ABSTRACT

A mechanical shear model for structural concrete members with and without stirrups is presented, which incorporates the most relevant shear transfer mechanisms. The model is based on the principles of structural mechanics, on a number of assumptions supported by the observed experimental behaviour and by the results of refined numerical models. Simple, direct and robust expressions are derived for shear strength verification and for design of the transverse reinforcement. The general theory behind the model enables it for steel or FRP simply supported or continuous, reinforced or prestressed concrete members, with any cross section, subjected to distributed and point loads or to axial forces. Excellent agreement between the results of a large number of shear tests and the model predictions has been obtained. The model is currently being extended to punching of slabs, for which the critical perimeter is obtained as a result of the model formulation

Keywords: Structural concrete, mechanical model, shear, design, assessment

1. INTRODUCTION

The response of reinforced and prestressed concrete members under shear and flexure is affected by the multi-axial stresses state, by the crack induced anisotropy, by the interaction between concrete and reinforcement and by the brittleness of the failure mode, among other phenomena. In addition, prestressing considerably modifies the stresses and strains fields, the cracking load and the cracks patterns, affecting not only the structural response at service but also the mode of failure and the ultimate capacity with respect to reinforced concrete members.

In order to predict such a complex behaviour, refined analytical and numerical models have been developed; however their applicability in daily engineering practice is still limited because their complexity in use, time consumption and dependency of the numerous input parameters required. On the opposite, some simple equations used in practice are semi-empirical, without a clear mechanical meaning, present large scatter and bias when compared with data bases of experimental results and cannot be easily updated to the technical advances (new materials, larger sizes, etc.). In new designs, scatter is accounted for by means of rather high safety factors; however, when assessing existing structures, some elements may be wrongly judged unsafe when using such empirical

[1] *Departamento de Ingeniería Civil y Ambiental. UPC Barcelona-Tech (ESPAÑA). antonio.mari@upc.edu (Corresponding author)*

[2] *Departamento de Física. Universitat de les Illes Balears (ESPAÑA). antoni.cladera@uib.es*

[3] *Departamento de Ingeniería Civil y Ambiental. UPC Barcelona-Tech (ESPAÑA). jesus.miguel.bairan@upc.edu*

[4] *Departamento de Ingeniería Civil y Ambiental. UPC Barcelona-Tech (ESPAÑA). eva.oller@upc.edu*

A unified mechanical model for design and assessment of concrete structures in shear and punching
Third International Conference on Mechanical Models in Structural Engineering
University of Seville. 24-26 june 2015.

equations outside their range of applicability, Ferreira, Bairán & Marí [1]. Furthermore, empirical approaches difficult the application of the performance-based-design paradigm.

In the last decade, advances in analytical and numerical models of concrete beams under shear stresses have been produced, Vecchio & Collins [2], Vecchio [3], Bairan & Marí [4] and [5], Petrangeli, Pinto & Ciampi [6], Bentz [7], Navarro-Gregori et al [8], Saritas and Filippou, [9], Mohr, Bairán & Marí [10], Ferreira, Bairán & Mari [1]. Particularly, it is possible to account for crack-induced anisotropy and cross-section distortion, which demonstrate the migration of shear stresses through the cross-section or the effects of the section's shape, among other aspects. These models have contributed to a better understand the evolutionary nature of the phenomenon and the experimentally observed behaviour.

In addition, simplified models for the shear strength of reinforced and prestressed concrete members have been developed, with the purpose of providing useful formulations for the daily engineering practice. The most relevant among them, are those carried out by Reineck [11], Zararis & Papadakis [12], Choi, Park and Wight [13], Tureyen & Frosch [14], Muttoni & Ruiz [15], Park, Kang & Choi [16], Wolf & Frosch [17], Collins, Bentz, Sherwood &Xie [18], Recupero, D'Aveni & Ghersi,[19], some of which have been included in codes provisions, such as the CAN/CSA-A23.3-04 (R2010) [20] or the FIB Model Code 2010 [21]. Other codes have incorporated empirical formulations, such as the ACI Building Code [22] and the Eurocode for concrete structures [23], especially for beams without stirrups. Nevertheless, the shear strength of structural concrete elements is still an open topic as no universally accepted formulation is available yet, capable to combine accuracy, simplicity and capacity to by adapted or extended to many different situations without the need for adjustments to existing or new experimental results. Furthermore, some questions related to the shear behaviour and strength can be raised, which are not clearly answered by the existing simple formulations, such as:

• Is the concrete contribution Vc, independent on the load level, on the presence of transverse reinforcement or on existing tensile forces (i.e. due to constrained shrinkage)?

• In continuous beams, do regions near the end supports (M≅0) resist the same shear as regions near the intermediate supports (M>>0)?

• What's the contribution of flanges to the shear strength of beams with T or I cross section?

• How the type of load (concentrated, distributed) affects the shear strength?

• If some shear mechanism depends on tensile strength, why f_{ct} does not play almost any role in the current codes shear resistance formulations for cracked beams?

• In post-tensioned concrete members, which is the effective depth to use in the shear strength calculations, d_p (prestressing tendon) or d_s (longitudinal mild steel reinforcement)?

• Why and how much the longitudinal reinforcement influences the shear strength?

• Where the critical shear crack forms and what are the factors influencing its position?

• What's the physical meaning of the slab punching critical perimeter around a column?

In order to answer these and other similar questions in daily engineering practice, simple but accurate models supported by a theory capable to capture the physics of the shear response are needed.

Recently, a mechanical model for the prediction of the shear strength of reinforced and prestressed concrete beams with rectangular, I or T shaped sections (Marí et al [24] and [25], Cladera et al [26] with or without transversal reinforcement was developed by the authors and experimentally verified with a large data base of shear tests results. Simple analytical expressions were obtained for the

contribution of the main shear resisting actions at the limit situation of shear failure. The predictions of the model were compared against different code formulation and large databases already published by Reineck et al. [27], [28] and [29], showing small bias and dispersion, and good correlation of the evolution of the different design parameters. These characteristics make the model particularly adequate for design, assessment of existing structures, and reliability analysis Furthermore, the rational basis of the approach allows analytical extensions to other applications with physical interpretation of the observed differences, such as FRP-reinforced or prestressed concrete, the effects of axial tension or compression loads, of transverse or vertical prestressing forces introduced by means of bars or stirrups, the shear strength of composite precast prestressed and cast in place concrete members and other possibilities. In this paper, the basis of this shear strength model is explained and used to answer the above raised questions. In addition the methodology for the extension to punching failure of slabs is explained, providing some promising preliminary results.

2. DESCRIPTION OF THE MODEL

2.1 Basic assumptions

According to ASCE-ACI Committee 445 [30], the shear strength in a RC beam is provided by a) the shear resisted by the un-cracked concrete chord; b) the friction and residual tensile forces developed along the crack length c) the shear strength provided by the transverse reinforcement and e) the dowel action at the longitudinal reinforcement. Under incremental loading, flexural cracks are formed which develop inclined along the web, Fig.1. During a relatively large portion of the load history, significant fraction of the shear force is transferred through the inclined cracked by means of aggregate interlock and residual tensile stresses, both produced by the bridging of stresses through aggregate and the un-cracked concrete in the meso-scale. However, while loading increases, the critical crack width increases; hence, this action tends to soften and redistribution of shear stresses to other softening mechanism takes place depending on the internal equilibrium conditions and their relative stiffness. In general, the shear stresses in the compression chord, which has remained uncracked during most part of the loading, tend to increase. Therefore, the compression chord will be subjected to a multiaxial stress state consisting in at least axial compression and shear.
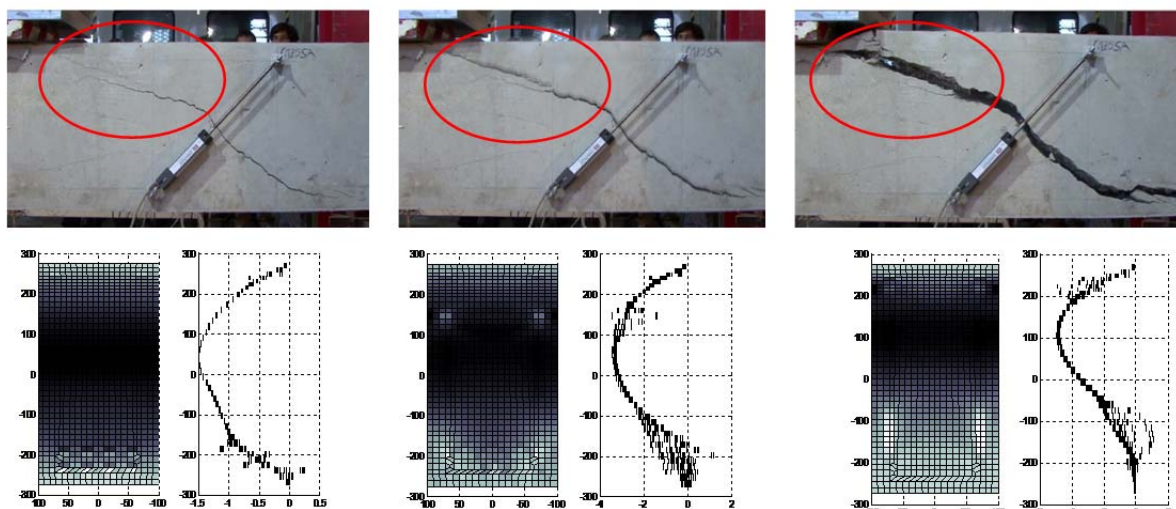

Figure 1. *Critical crack evolution and numerical prediction of shear stresses under shear loading.*

A unified mechanical model for design and assessment of concrete structures in shear and punching
Third International Conference on Mechanical Models in Structural Engineering
University of Seville. 24-26 june 2015.

Eventually, a new crack takes place and develops above the neutral axis trough the compression chord, in the point that first reaches the concrete strength under multiaxial stresses state initiating softening of the compression chord. At the same time, tensile shift in the longitudinal reinforcement increases, which may produce bond cracks in the bottom reinforcement. If premature bond failure does not take place, failure of the element will be controlled by the shear capacity of the compression chord as it is the last element that typically initiates softening. Resistance of compression head is assumed to be governed by Kupfer's biaxial failure envelope. It is considered that failure occurs when the principal stresses reach the Kupfer's compression-tension branch of the failure surface [31].
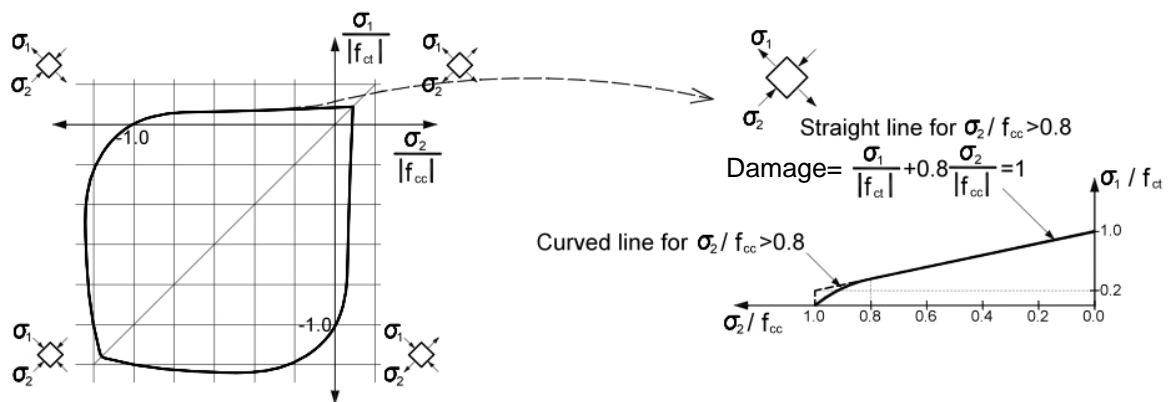

Figure 2. *Adopted failure envelope for concrete under a biaxial stress state.*

In the present model, it is considered that the total shear resistance, Eq. (1), is the sum of the shear resisted by concrete (V_c) and by the transverse reinforcement (V_s). V_c is explicitly separated into the following components, whose importance are considered to be variable as damage propagates: shear resisted in the uncrack compression head (V_c), shear transfer across web cracks (V_w) and the contribution of the longitudinal reinforcement (V_l). Note that here V_c represents the shear in the compression chord of the beam, not the total concrete contribution to shear.

$$V = V_c + V_w + V_l + V_s = f_{ct} \cdot b \cdot d \cdot \left(v_c + v_w + v_l + v_s \right)$$

(1)

Lower case variables v_c, v_w, v_l and v_s are the dimensionless values of the shear transfer actions. As the crack width increases, the aggregate interlock and residual tension soften and an increase in the shear transferred by the compression concrete chord takes place. Hence, it will be assumed that at the limit state, previous to incipient failure, the shear stress distribution in the critical section is similar to the one represented in Fig. 3; where the approximated distribution of each contributing action is also indicated, x is the neutral axis and d the effective depth of the section. Notice that here the stage just prior to the formation of the crack in the compression chord is considered. This stress profile is a qualitative distribution of the stresses in a section close to that of the tip of the first branch of the critical crack and it is not affected by the local state of stresses around the tip. In developing the design formulation, the following additional simplifications are also considered: The distribution of normal compressive stresses in the un-cracked zone will be then considered linear; hence, the position of the neutral axis can be computed as that of a cracked section in elastic range regime.
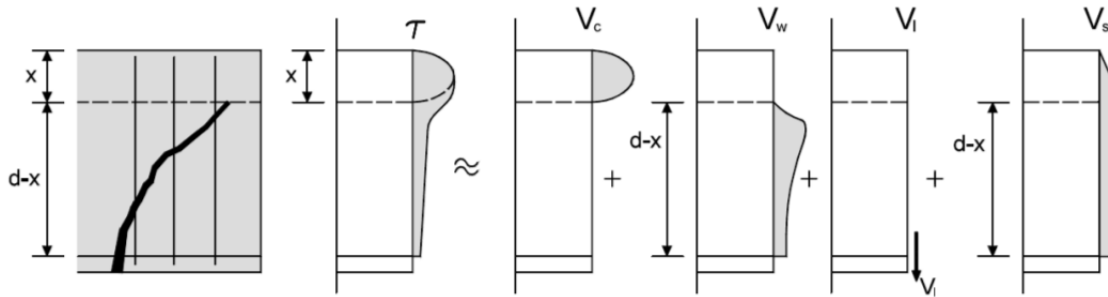
Figure 3. *Qualitative distribution of shear stresses at imminent shear failure and distribution.*

Based on experimental and numerical observations, the mean crack inclination is approximated as function of the relative neutral axis depth (x/d), in Eq. (2), valid for rectangular, T or I sections. Where K_θ is a coefficient that takes into account the change of crack inclination in a section with flanges, see Fig. 4; hence, in this case Eq. (2) refers to the inclination of the secant of the crack from the longitudinal reinforcement to the neutral axis. K_θ is computed by Eq. (3), it takes value 1 for rectangular sections or when x≥hf.

$$\cot\theta = \frac{0.85}{1-\frac{x}{d}}K_\theta \tag{2}$$

$$K_\theta = \frac{(d-h_f)+(h_f-x)\frac{b}{b_w}}{d-x} \geq 1 \tag{3}$$
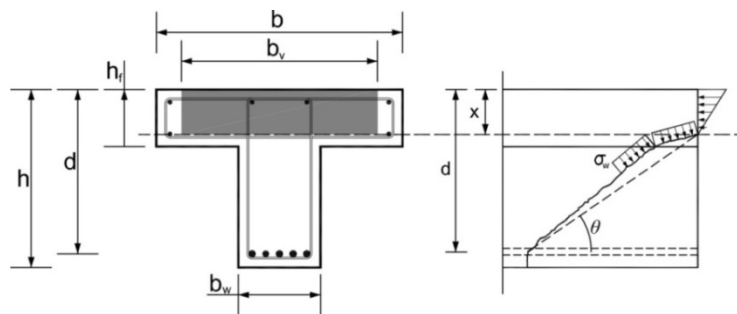
Figure 4. *Change of crack inclination when entering the flange.*

The weakest section in front of a combined shear-bending failure is considered to be placed at the tip of the first branch of the critical crack for beams with constant geometry and reinforcement (Fig. 5). Any other section closer to the zero bending moment point has a bigger depth of the compression chord, produced by the inclination of the crack and will resist a bigger shear force. Any other section placed farther from the support will have the same depth of the compression chord but will be subjected to higher normal stresses and, therefore, will have a higher shear transfer capacity.

When load is increasingly applied, flexural cracks successively appear as the bending moment increases, whose spacing depends basically on tensile concrete and bond properties (Fig. 5). It is assumed that the critical crack is the closest crack to the zero bending moment point and that it starts where the bending moment diagram at failure reaches the cracking moment of the section, resulting $s_{cr} = M_{cr}/V_u$, which is a conservative assumption.
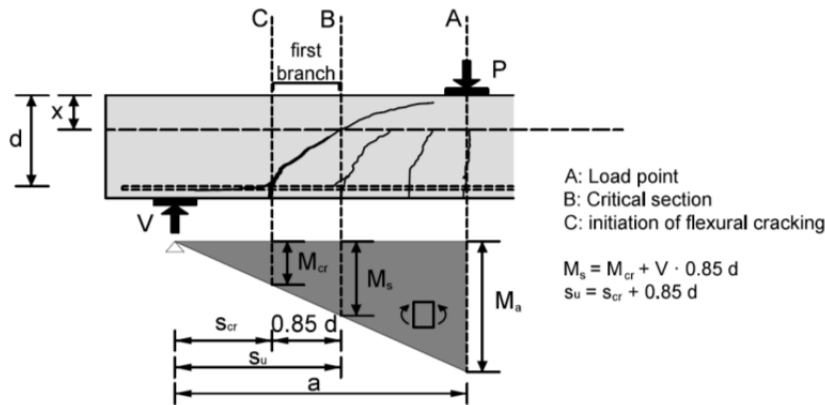
A unified mechanical model for design and assessment of concrete structures in shear and punching
Third International Conference on Mechanical Models in Structural Engineering
University of Seville. 24-26 june 2015.

Figure 5. *Position of the shear critical section in the beam.*

When stirrups are anchored in the compression zone, they collaborate in the strength of the compression head by producing a confining vertical compression (σ_y) at depth larger than the concrete cover (d'), see Fig. 6, of value given by Eq. (4):

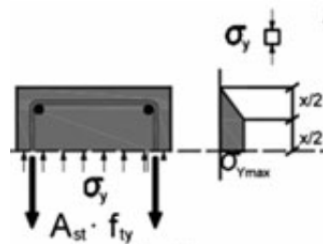$$\sigma_y = \frac{A_{sw} \cdot f_{yw}}{b} = \rho_w f_{yw} \tag{4}$$

Figure 6. *Confinement stresses introduced by the stirrups in the un-cracked concrete zone.*

2.1. Contribution of cracked concrete web (V$_w$)

Shear resistance of cracked concrete in the web is considered as the residual tensile stress of cracked concrete. The mean tensile stress of the softening curve is considered distributed in a depth x_w of the cracked zone of the cross-section where the tensile σ-ε curve reaches zero tension, see Fig. 7. A linear softening branch of the σ-ε curve has been assumed which is consistently dependent on the fracture energy in mode I (G_f).

By setting the geometrical relationship between the crack opening at the level of the longitudinal reinforcement and at the point of the crack where the residual tensile stress is zero, and relating the crack opening to the reinforcement longitudinal strain ε_s and the crack spacing, the shear transferred along the closest part of the crack can be expressed in function of ε_s. Then, to obtain a simple design equation the following average values are conservatively assumed: longitudinal reinforcement strain when shear failure occurs, ε_s=0,0009, angle of the struts θ=36º, which corresponds to a mean longitudinal reinforcement ratio of ρ=1,5 %, resulting the following value for v_w:

$$v_w = 0.425 \, \frac{\varepsilon_{ctu}}{\varepsilon_s} \sin^2\theta \cong 167 \frac{f_{ct}}{E_c}\left(1 + \frac{2E_c G_f}{f_{ct}^2 d}\right) \tag{5}$$

The concrete tensile strength (f_{ct}) is evaluated as the mean tensile strength according to Eurocode 2 [24], but limiting the concrete compression strength to 60 MPa for the elements without stirrups in order to account to the possible fracture of the aggregate in high-strength concrete. G_f is the fracture energy of concrete which depends on the concrete strength and the aggregate size, computed as shown in Eq. (9).

$$G_f = 0.028 \cdot f_{cm}^{0.18} \cdot d_{max}^{0.32}$$

(6)

A more detailed derivation of the equation is carried out in [1]. In the case of T or I shaped sections, it is accepted that the shear transferred along the crack takes place mainly in the web, so the web width "b_w" should be used when computing the absolute V_w in Eq. (1), i.e. $V_w = v_w\, f_{ct}\, b_w\, d$.
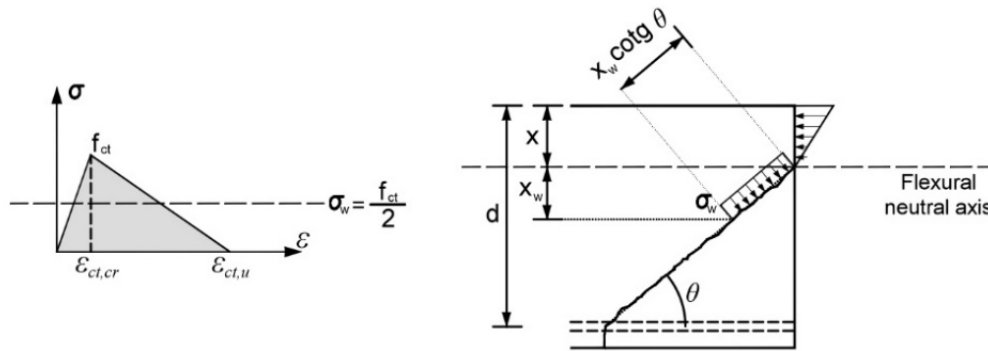
Figure 7. *Contribution of cracked concrete to shear resistance.*

2.2. Contribution of the longitudinal reinforcement (Dowel action, V_l)

Contribution of longitudinal reinforcement, or dowel action, is considered by the model only when there are stirrups, as they provide a constraint to the vertical movement of the longitudinal bars, enabling them to transfer shear. In order to evaluate such shear force, it is considered that the longitudinal bars are doubly fixed at the two stirrups adjacent to the crack initiation, and subjected to bending due to a relative imposed displacement between those points. This vertical relative displacement is considered caused by the critical crack opening and by the shear deformation of the compression chord. This contributing component clearly depends on the tensile steel ratio which is implicitly represented by means of the x/d parameter. A simplified expression is presented in Eq. (7)

$$v_s > 0 \rightarrow v_l = 0.23\,\frac{n\rho}{1 - x/d}$$

(7)

2.3. Contribution of transversal reinforcement (V_s)

Contribution of transversal reinforcement, Eq. (8) is taken as the integration of the forces in the stirrups cut by the inclined crack up to a height of (d-x), see Fig. 3, and assuming that transversal reinforcement is yielded along the total crack height.

$$v_s = 0.85 \rho_w \frac{f_{yw}}{f_{ct}}$$

(8)

A unified mechanical model for design and assessment of concrete structures in shear and punching
Third International Conference on Mechanical Models in Structural Engineering
University of Seville. 24-26 june 2015.

2.4 Contribution of the compression chord (V_c)

It is stated that the shear resisted in the compression chord starts softening when the most critical fiber reaches the Kupfer's failure envelope, assuming a linear distribution of longitudinal stresses produced by existing bending moment, and a transversal confining stresses provided by existing stirrups. The position of the failure point depends on the ratio between bending moment and shear force (M/Vd). A study performed in [24] shows that for values of M/Vd less than 3 (which is usually the position of the critical shear section), the point where failure initiates is placed at a distance from the neutral axis around $\lambda=0{,}425x$, being "x" the depth of the compressed zone.

By means of a Mohr's circle analysis, Eq. (9) can be derived, where σ_x is the normal stress in the most critical fiber, located at position $\lambda \cdot x$ from the bottom of the neutral axis. K_λ is a parameter relating the mean shear stress in the compression chord with stress in the critical fiber; therefore, it depends on the shape of the distribution of shear stresses in the compression chord (Fig. 3), and on the position of the critical fiber. The distribution of longitudinal stresses can be related to the applied bending moment, and the confining stresses can be derived from the contribution of the transversal reinforcement to the shear resistance, according to Eq. (4).

$$v_c = \frac{1}{f_{ct}} \zeta K_\lambda \frac{x}{d} \sigma_1 \sqrt{1 - \frac{(\sigma_x+\sigma_y)}{\sigma_1} + \frac{(\sigma_x\sigma_y)}{\sigma_1^{2}}} \tag{9}$$

Therefore, by setting the equilibrium equations between the internal forces and the stress resultants, see Fig. 8, Eq. (9) can be expressed as Eq. (10).

$$v_c = R_t K_\lambda \zeta \frac{x}{d} \sqrt{1 - \frac{2\lambda(0.2+0.85v_c+v_w z_w+0.425v_s)}{\frac{x}{d}\left(1-\frac{x}{3d}\right)R_t}\left(\frac{v_s}{0.85R_t}-1\right) - \frac{v_s}{0.85R_t}} \tag{10}$$

Where ζ is the size effect parameter for the compression head (Eq. 11), which can be assimilated to that of a splitting test, as proposed by Zararis and Papadakis [12].

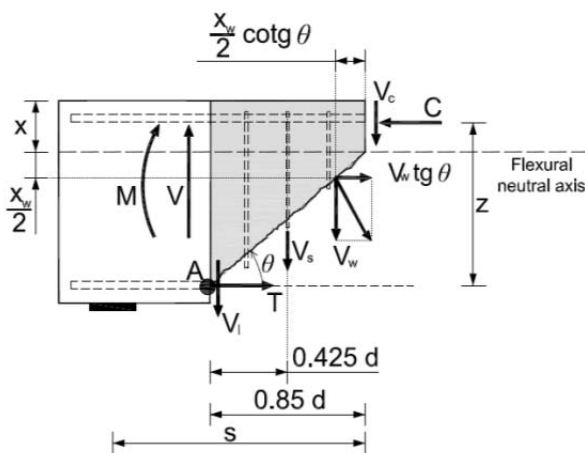$$\zeta = 1.2 - 0.2 \cdot a \geq 0.65 \quad \text{(a in meters)} \tag{11}$$

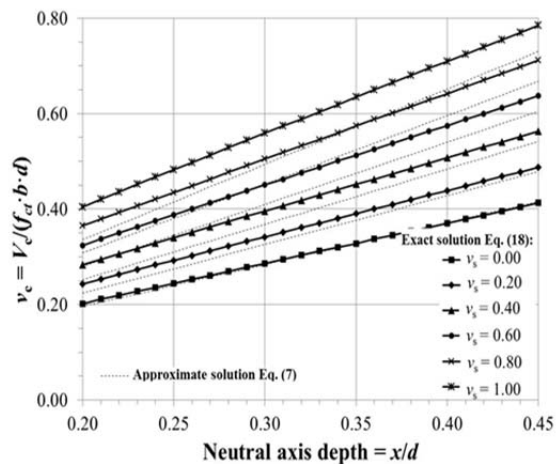**Figure 8.** *Internal forces in PC beam portion.*

Figure 9. *Uncracked concrete contribution to shear.*

It is observed that v_c depends on v_s and that Eq. (10) is a recurrent equation, since R_t (strength reduction factor due to the biaxial stress state) is not known a priori; hence, in general, an iterative procedure is required to find the resisted v_c. ¡However, after an extended parametric study, it can be observed that v_c is almost linear with x/d. Therefore, for practical purposes, Eq. (12) is proposed as a linearization of Eq. (10). In Fig. 9, the exact solution of Eq. (10) is compared with the simplified linearization of Eq. (12) in dashed lines, for the case of a rectangular section.

$$v_c = \zeta \left[\left(0.70 + 0{,}18 Kt_t + \left(0.20 + 0.50 \frac{b}{b_w} \right) v_s \right) \frac{x}{d} + 0.02 K_t \right] \tag{12}$$

In the case of T or I beams, the shear stresses at the un-cracked zone are concentrated in the flanges near the web. Terms b and b_w are the width of the flange and the web respectively, as defined in Fig. 3. While $b_v{}^*$ is the effective flange width in which shear stresses can be considered distributed in the compression flange. In the case of rectangular sections $b_v{}^*=b=b_w$; while for T and I sections, $b_v{}^*$ can be computed as shown in Eq (13.1) and (13.2)

$$x \le h_f \rightarrow b_v = b_w + 2h_f \le b \tag{13.1}$$

$$x > h_f \rightarrow b_v = b \left[v^2(3 - 2v) + \frac{b_w}{b}(1 - 3v^2 + 2v^3) \right]; \ v = \frac{h_f}{x} \tag{13.2}$$

Where the neutral axis depth "x" must be calculated accounting for the geometry of the T or I section, as is proposed in [27]. In addition, K_T is a coefficient to take into account the different cracking moment of a T beam with respect to a rectangular one with $b=b_w$ and equal depth rectangular and a T beam, computed by Eq. (14).

$$K_T = \frac{M_{cr,T}}{M_{cr,R}} \frac{b_w}{b} \approx 0.9 \frac{b_w}{b} + 0.1 \tag{14}$$

After parametric studies it has been found that both K_θ and K_T have very small influence on the global shear strength so that for the sake of simplicity they will be set to unity.

2.5 Contribution of prestressing

The most significant effects of prestressing on the shear behavior are:

- Changes the principal tensile and compressive stresses and the angle θ of the cracks with respect to the longitudinal. Cracking can be avoided (total prestressing) or limited below a certain crack width (partial prestressing). At high loading levels, flexural cracks in zones where bending moments are low, can be eliminated thus resulting only inclined cracks at the web due to shear. In members with thin webs, the risk of concrete crushing increases.
- Increment of the flexural neutral axis depth, thus increasing the contribution of the compressive concrete chord. The neutral axis depth depends on the force, eccentricity and inclination of the prestressing force and on the external moment at the considered section.
- In case of inclined tendons, the vertical component of the prestressing force, $V_p=P\cdot\sin\alpha$ helps to resist the external shear.
- Increment of the cracking moment of the section what modifies the position where the critical crack initiates and the position of the critical section, which is displaced farther from the zero bending moment point in comparison with RC structures. Therefore, the bending moment at the

A unified mechanical model for design and assessment of concrete structures in shear and punching
Third International Conference on Mechanical Models in Structural Engineering
University of Seville. 24-26 june 2015.

critical section increases and, consequently, the shear resisted by the compressed concrete chord.

- Reduction of crack width, thus incrementing the aggregate interlock along the crack
- In case of bonded tendons, the crack opening increments the stress at the tendons, as in the case of mild reinforcement, helping to resist shear and flexure.

The inclusion of each of the above aspects on the above described mechanical model developed for RC structures will be explained next.

2.5.1. Neutral axis depth in cracked prestressed concrete sections

Let's consider a section with active (prestressed) and passive (non-prestressed) reinforcements subjected to a bending moment M and a prestressing force P with an eccentricity "e", see Fig. 10.
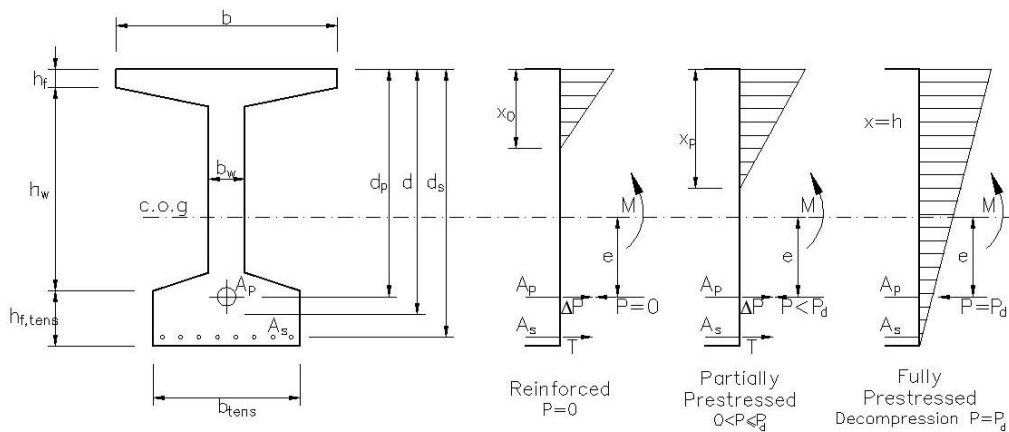
Figure 10. *Interpolation of neutral axis depth between reinforced and fully prestressed concrete*

To take into account different reinforcement arrangements in a cross section (only mild reinforcement, only active reinforcement or both), the effective depth is defined as the distance from the center of gravity of the existing reinforcement bars to the most compressed concrete fiber:

$$d = \frac{A_s d_s + A_p d_p}{A_s + A_p} \tag{15}$$

The consideration of an axial load in the equilibrium of normal forces and bending moments produces coupling between both equations. As a result, the neutral axis depth depends on the mild and prestressing reinforcement amounts, on the bending moment, on the prestressing force and on its eccentricity, so its computation is not straightforward. For practical purposes, a linear interpolation is made between the neutral axis depth"x_0" obtained for the same reinforcement amounts, considering P=0, and for the decompression force, P=P_d, for which the neutral axis depth is x=h. The prestressing decompression force P_d is the force that, for a given eccentricity "e" and acting external moment M, would produce zero stress at the extreme concrete fiber of the tensile zone, see Fig. 10. The interpolation equation for the relative neutral axis depth, ξ=x/d is, then:

$$\frac{x}{d} = \frac{x_0}{d} + (\frac{h}{d} - \frac{x_0}{d})\left(\frac{d}{h}\right)\frac{Pc}{M - Pe} = \frac{x_0}{d} + (\frac{h}{d} - \frac{x_0}{d})\left(\frac{d}{h}\right)\frac{\sigma_{cp}}{\sigma_{cp} + f_{ct}} \tag{16}$$

In which the moment considered is the cracking moment, and σ_{cp} is the mean concrete stress produced at the section by prestressing, $\sigma_{cp}=P/A_c$. Eq. (16) has been compared with the theoretical solution by solving the non-linear system of coupled equations, for a large number of cases covering different levels of prestressing (σ_{cp}/f_{ct}), eccentricities (e/c) and non-prestressed neutral axis depth x0, obtaining quite good approximation for usual cases and, therefore, will be adopted in this study to obtain x/d.

2.5.2. Inclination, horizontal projection and position of the critical shear crack

The critical crack initiates at the most tensioned concrete fibre, and starts inclining where it reaches the mild reinforcement, so the same value for the horizontal projection of the crack, $0,85d_s$ is adopted for prestressed concrete members. The cotθ of the shear critical crack angle for prestressed concrete members will be higher than in reinforced concrete because the higher neutral axis depth:

$$\cot\theta = \frac{0.85d_s}{d_s - x} \tag{17}$$

In prestressed members without longitudinal mild reinforcement ($A_s=0$), it can be adopted $d_s=h$. The model assumes that the critical shear crack initiates in the section where the bending moment, at shear failure, reaches the cracking moment. Thus, the higher is the cracking moment, the farther is the position of the crack with respect to the zero bending moment section.
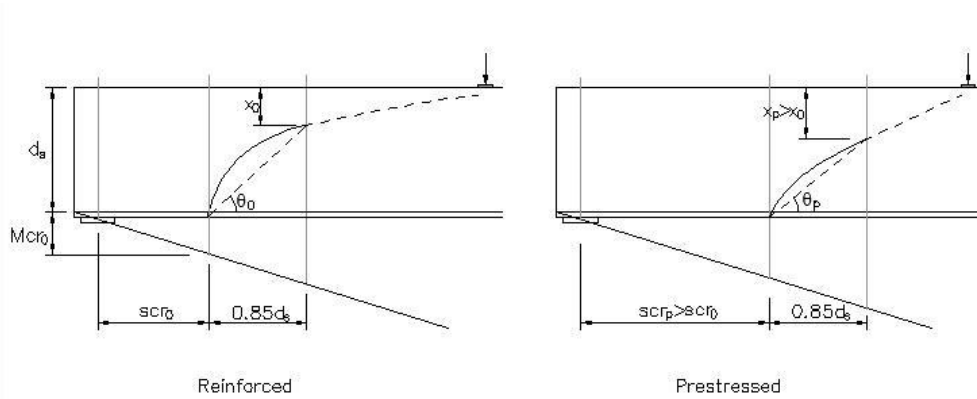
Figure 11. *Position of the shear critical crack in reinforced and in prestressed concrete members.*

2.5.3. Shear Transferred across the crack

The shear transferred across the crack, due to residual tensile stresses is given by:

$$v_w = 0.425 \frac{\varepsilon_{ctu}}{\varepsilon_s} sin^2\theta \cong 167 \frac{f_{ct}}{E_c}\left(1 + \frac{2E_c G_f}{f_{ct}^2 d}\right) \tag{18}$$

For pre-stressed concrete members, the angle of inclination of the cracks given by Eq (17) should be adopted. In addition, the effect of prestressing on the crack opening is considered by subtracting the average concrete strain due to prestressing $\varepsilon_{cp}=\sigma_{cp}/E_c$ from the longitudinal reinforcement strain, ε_s whose average value, as previously mentioned, can be estimated as ε_s =0,0009. For P=0 ($x_p=x_0$; $\varepsilon_{cp}=0$) the above expression is identical to that derived for reinforced concrete

2.5.4. Dowel action.

A unified mechanical model for design and assessment of concrete structures in shear and punching
Third International Conference on Mechanical Models in Structural Engineering
University of Seville. 24-26 june 2015.

In the case of prestressed concrete members, only mild reinforcement supported on the stirrups is considered to produced dowel action. Therefore, the same simplified expression than in reinforced concrete is used, excluding the prestressing tendons when calculating the reinforcement ratio and the neutral axis depth in Eq. (7).

2.5.5. Concrete contribution in prestressed concrete member

Consider the portion of a beam placed over the inclined crack, as indicated by Figure 12. The prestressing force (with its inclination and eccentricity) takes part in the equilibrium of forces and moments (taken with respect to the point where the crack is crossed by the longitudinal reinforcement "d_s"). In Fig.12, ΔP is the increment of force in the active reinforcement due to the crack opening, which will be neglected in this work.
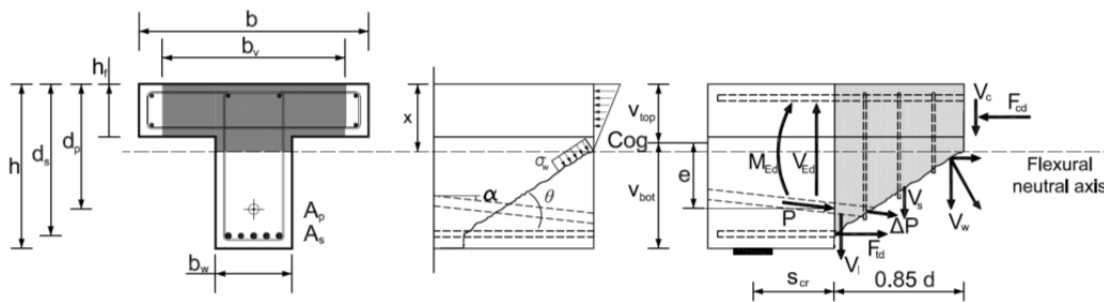
Figure 12. *Forces acting on a rigid body part of a beam placed over the critical shear crack.*

Assuming that, at failure, the moment at the crack initiation is the cracking moment of the prestressed section, $M_{cr,p}$ and grouping the moments due to prestressing, and following the same procedure than in reinforced concrete, Eqs. (9) and (10), the following equation is obtained , for the shear transferred by the uncracked compression zone in prestressed concrete:

$$v_c = R_t K_\lambda \zeta \frac{x}{d} \sqrt{1 - \frac{2\lambda(\mu + 0.85v_c + v_w\beta_w + 0.425v_s)}{\frac{x}{d}\left(1 - \frac{x}{3d}\right)R_t}\left(\frac{v_s}{0.85R_t} - 1\right) - \frac{v_s}{0.85R_t}} \qquad (19)$$

Where μ is the dimensionless bending moment with respect to the mild reinforcement, at the section where the critical crack initiates, see Fig. 12, when shear failure occurs.

$$\mu = \mu_{cr0} + \mu_p \quad ; \quad \mu_{cr0} = \frac{M_{cr0}}{f_{ct}bd^2} \quad ; \quad \mu_p = \frac{P\cos\alpha\,(c + d_s - d_p)}{f_{ct}bd^2} \qquad (20)$$

$M_{cr,0}$ is he cracking moment of the section without considering the prestressing force and β_w is the non-dimensional lever arm of the residual tensile force transferred along the crack, with respect to the point where moments are taken.

2.5.6. Simplified equations for the concrete contribution to shear strength of prestressed concrete beams

The main difference between Eq. (20) and Eq. (10) is the moment at the section where the crack initiates, which is affected by prestressing. In fact, Eq. (19) can be linearly expressed by Eq. (21), which is the same than Eq (12), making $K_T = K_\theta = 1$, but affected by a factor which depends on the bending moment μ, as indicated by Eq (22):

$$\upsilon_c = \frac{b_{v,eff}}{b_f}\left\{\left(0.88+\left(0.20+0.50\frac{b_f}{b_w}\right)\upsilon_s\right)\frac{x}{d}+0.02\right\}\left[0.94+0.3\mu\right] \tag{21}$$

By substituting $\mu = \mu_{cr0} + \mu_p$, and taking into account that the dimensionless cracking moment of a rectangular cross section is 0.2, Eq. (21) can be rewritten as a function of μ_p (see Eq. 20) which is a function of the prestressing force and position:

$$\upsilon_c = \frac{b_{v,eff}}{b_f}\left\{\left(0.88+\left(0.20+0.50\frac{b_f}{b_w}\right)\upsilon_s\right)\frac{x}{d}+0.02\right\}\left[1+0.3\mu_p\right] \tag{22}$$

The right parenthesis will be called K_p, a factor which takes into account the increment of cracking moment in a prestressed concrete section, with respect to a reinforced concrete one; $b_{v,eff}$ is the effective width for the shear strength transferred by the compression chord, given by Eqs. (13.1) and (13.2) Particularizing the expression (22) for P=0 and/or for ($b_v=b_w=b$), identical equations than those derived for reinforced concrete or for rectangular sections are obtained, respectively.

The total shear resisted by a prestressed concrete beam is, accounting for the tendon inclination:

$$V = V_c + V_s + P\sin\alpha \ ; \ \ V_c = \left(\upsilon_c + \upsilon_w + \upsilon_l\right)f_{ct,d}\,bd \ ; \ \ V_s = \frac{A_{st}}{s_t}f_{ywd}\left(d_s - x\right)\sin\alpha\left(\cot\theta + \cot\alpha\right) \tag{23}$$

3. SIMPLIFIED EQUATIONS IN A CODE-TYPE FORMAT

The described model provides the contribution of each shear transfer action; however, for design purposes, some simplifications are still necessary in order to make the model easier to use in daily engineering practice. Then, taking into account that when shear-flexure failure takes place, both the aggregate interlock and the dowel actions are small compared to the shear resisted by the uncracked zone, v_w and v_l have been incorporated into v_c. For this purpose, the following average values have been adopted: v_w=0.035, v_l=0.025, vs=0.25 and x/d=0.35. Then, term $(v_w+0,02)/0.35=0,157$ has been added to 0.88 and the dowel action term $v_l/(0,35\cdot0,25)$, which only exists when $A_{st}>0$ has been added to the factor multiplying v_s in Eq (22), resulting in the following compact equation:

$$V_{cu} = \zeta\frac{x}{d}K_p\left[0.30\frac{f_{ck}^{2/3}}{\gamma_c} + 0.5\left(1+\frac{b}{b_w}\right)\frac{v_{su}}{b\cdot d}\right]b_{v,eff}d \tag{24}$$

where the mean concrete tensile strength has been expressed in terms of the characteristic concrete compressive strength, f_{ck}, affected by the corresponding safety partial coefficient, and K_p is the factor which takes into account the effects of the axial load, including prestressing, (compression positive), and the interaction with the bending moment acting at the considered section:

$$K_p = 1 + 0.24\frac{P\,y_t+M_v}{f_{ctm}bd^2} \tag{25}$$

y_t is the distance from the c.o.g. of the section to the most stressed fibre in tension and M_v is the excess of moment with respect to the cracking moment at the considered section. Equation (24) is also valid for members subjected to a moderate axial compressive load, such as some columns, and can be extended to members under tensile axial forces or with constrained imposed deformations.

A unified mechanical model for design and assessment of concrete structures in shear and punching
Third International Conference on Mechanical Models in Structural Engineering
University of Seville. 24-26 june 2015.

Shear reinforcement is necessary when the shear design force exceeds the shear resisted by the concrete, without transverse reinforcement, V_{cu0},

$$V_{cu0} = 0.30\zeta \frac{x}{d} K_p \frac{f_{ck}^{2/3}}{\gamma_c} b_{v,eff} d \tag{26}$$

$$V_{su} = \frac{V_{Ed} - V_{cu0}}{1 + 0.5\zeta \frac{x}{d} K_p \left(1 + \frac{b}{b_w}\right) \frac{b_{v,eff}}{b}} \tag{27}$$

It is observed that due to the confinement of the concrete uncracked concrete zone produced by the stirrups, the amount of transverse reinforcement is reduced (denominator >1)

4. VERIFICATION OF THE MODEL WITH SHEAR TESTS RESULTS

Table 1 shows a comparison of the model predictions with the results of a large set of shear tests of reinforced and prestressed concrete beams, with rectangular, I or T sections. It is observed that very good agreement is in general obtained and, especially, for reinforced concrete beams. In addition, it can be observed that the Eurocode EC2 provides much large scatter in all cases, specially for prestressed concrete members

Table 1. Verification of the proposed model for different databases (V_{test}/V_{pred})

Database original source	Comments	No. elements	Mean		CoV (%)	
			Proposed	EC2	Proposed	EC2
Reineck & al (2013)	RC beams w/o stirrups	784	1.16	1.10	18.80	27.90
Reineck & al (2014)	RC beams with stirrups	170	1.12	1.52	16.5	33.40
Reineck & al (2015)	PC beams w/o stirrups	214	1.10	1.57	22.60	30.1
Reineck & al (2015)	PC beams with stirrups	117	1.05	1.54	16.10	37.2

Figures 13 and 14 show, respectively, the ratio V_{exp}/V_{pred} for reinforced and prestressed concrete beams with and without stirrups.
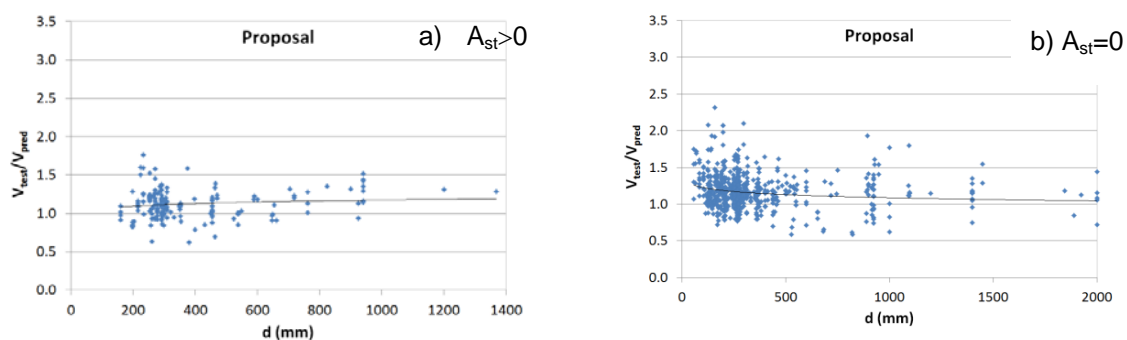
Figure 13. *Experimental validation of RC beams: a) with stirrups; b) without stirrups.*
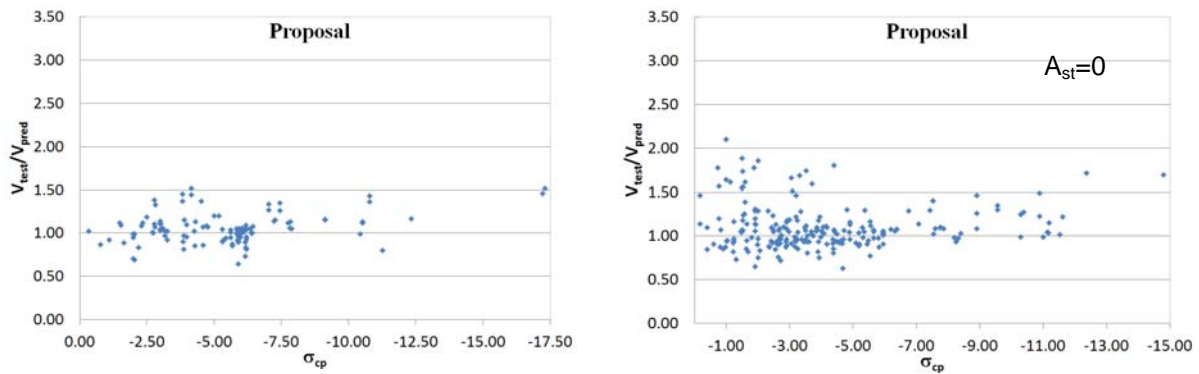
Figure 14. *Experimental validation of PC beams: a) with stirrups; b) without stirrups.*

Finally, Fig. 15 compare the results of the proposed method and those of EC2 for the total 1287 tests analysed. A big difference in the scatter can be observed. A mean of 1.13 and a Cov of 19.3% and a 5% real percentile of 0.839 are obtained for the proposed method while a mean of 1.27 a CoV of 35.5 % and a real 5% percentile of 0.804 are obtained for EC2, indicating that the proposed model is not only less disperse and more precise (less expensive) but also more safe.
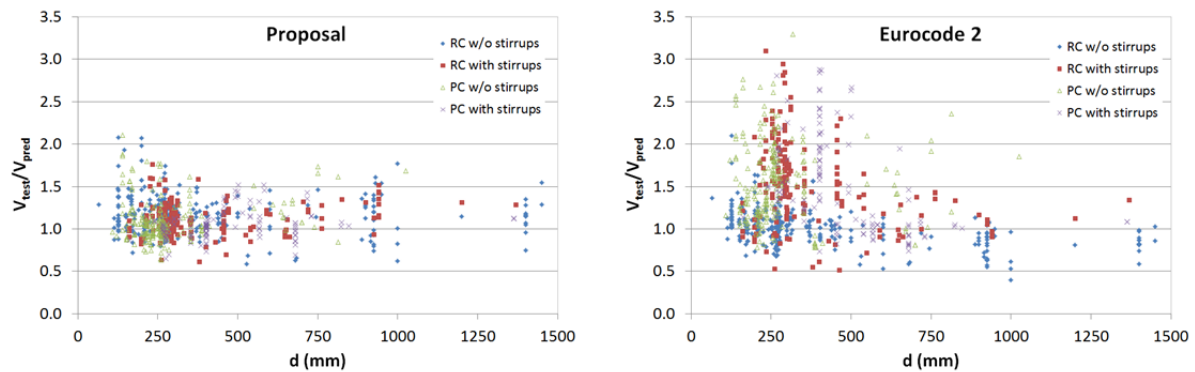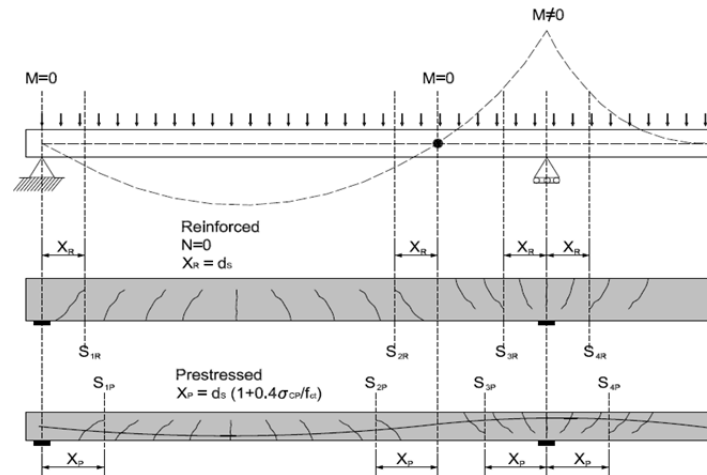

Figure 15. *Comparison of the total set of tests between the model and the EC2 predictions.*

5. EXTENSION OF THE MODEL TO OTHER SITUATIONS

5.1. Sections subject to bending moments $M_{Ed} >> M_{cr}$

Eq. (22) expresses the shear resisted by the uncracked concrete zone as a function of the bending moment at the section where the critical shear crack starts, thus accounting for the shear-bending interaction. Therefore it is useful for shear design or strength verification in sections where the bending moment is significantly bigger than the cracking moment. Such situation occurs, for example, where changes in the longitudinal or in the transverse reinforcement take place far from the zero bending moment point is.

Furthermore, near internal supports of continuous beams or in cantilevers, under distributed loads, the critical crack starts very near the support and not where the bending moment at failure equals the cracking moment, as it usually happens in positive bending moments zone. This is due to the fact that the maximum damage at the uncracked chord, according the failure criteria adopted (see Fig. 2), takes place near the support, since both the bending moment and the shear force increase as the control section approaches the support.
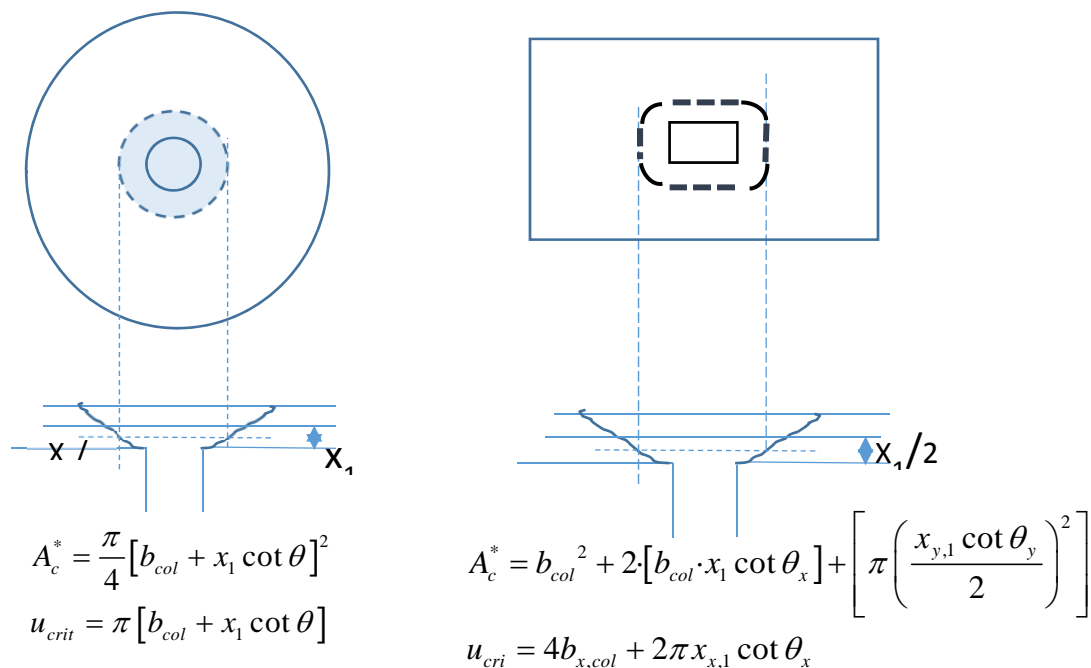
A unified mechanical model for design and assessment of concrete structures in shear and punching
Third International Conference on Mechanical Models in Structural Engineering
University of Seville. 24-26 june 2015.

Figure 16. *Sections to be checked in positive and negative bending moment zones.*

5.2. Punching in slabs around columns

The above considerations can be applied to the case of punching shear of slabs around the columns, since in this case the bending moment and the shear force increase as the section approaches the column, as shown in Fig. 16. The equation of the punching strength of slabs without transverse reinforcement can be obtained by adapting Eq. (26)

$$V_{cu} = \zeta \frac{x_1}{d} K_p \, 0.30 \frac{f_{ck}^{\frac{2}{3}}}{\gamma_c} u_{crit} d \qquad (28)$$

Where u_{crit} is the critical perimeter, which can be obtained by considering the failure point at the middle of the compression uncracked zone (depth $=x/2$), see Fig. 17. Therefore, the critical perimeter is a value inherent to the model formulation and depends on the amount of longitudinal reinforcement ratio.

$$A_c^* = \frac{\pi}{4} [b_{col} + x_1 \cot \theta]^2$$

$$u_{crit} = \pi [b_{col} + x_1 \cot \theta]$$

$$A_c^* = b_{col}^2 + 2 \cdot [b_{col} \cdot x_1 \cot \theta_x] + \left[\pi \left(\frac{x_{y,1} \cot \theta_y}{2} \right)^2 \right]$$

$$u_{cri} = 4 b_{x,col} + 2\pi x_{x,1} \cot \theta_x$$

Figure 17. *Critical perimeter in punching of slabs around circular and rectangular columns.*

Fig. 18 shows the preliminary results of this model when compared with the ACI punching database. For circular slabs the mean is 1,13 and the CoV 19,5%, while for square slabs the mean is 1,33 and the CoV is 20%. In the second case, furher refinements associated to the non-axisymmetric behaviour is needed
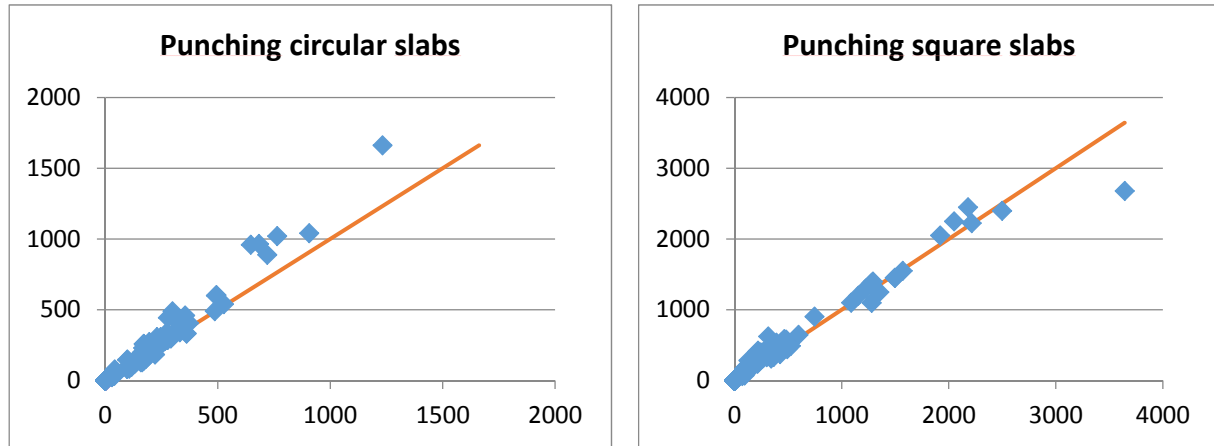
Figure 18. *Comparison between the model predictions and the ACI punching tests results*

5.3. Further extensions and adaptions of the model

Due to the mechanical bases of the model, it can be adapted to many different types of loading, materials, support conditions and even failure modes, just by identify the differences between the new situation and the existing one and by including them into the equations of the model.

For example, the model has been successfully adapted to FRP reinforced concrete beams with and without stirrups [32] and [33]. In these cases the following aspects were taken into account: 1) The FRP modulus of elasticity is much lower than that of steel and depend on the type of fiber used, so the aggregate interlock and the dowel action can be neglected and the ratio Er/Ec should be explicit in the formulation. 2) When FRP stirrups exist, it must be considered that they do ot yield, so their stress should be obtained from compatibility of strains along the inclined crack 3) sometimes stirrups break in the bent zone, which becomes the weakest point and, therefore, a limitation to the stirrups ultimate stress should be set.

Similarly, the model is being extended to beams subjected to loads near the supports, applied on the compression or tension sides, to moderately compressed columns with circular sections, and to steel fiber reinforced concrete beams, among other cases.

6. CONCLUSIONS

A mechanical model developed for the prediction of the shear-flexural strength of reinforced and prestressed concrete members with and without transverse reinforcement has been described and verified with a large data base. The model, which is valid for beams with I, T or rectangular cross sections, accounts for the generally accepted most significant shear transfer actions. The following conclusions can be drawn from the results provided by the model:

A unified mechanical model for design and assessment of concrete structures in shear and punching
Third International Conference on Mechanical Models in Structural Engineering
University of Seville. 24-26 june 2015.

1. Simple and direct expressions have been derived both for design of the transverse reinforcement and for the shear strength verification, which include the most relevant parameters governing the structural behaviour, thus resulting of great interest both for design and assessment of existing structures.

2. The shear transferred by the concrete compression chord near the limit point has been found to be very relevant in the derived model, and linearly dependent on the relative flexural neutral axis depth, x/d, which is a function of $n\rho$, being $n=E_s/E_c$ the modular ratio and $\rho=A_s/(b \cdot d)$ the longitudinal reinforcement ratio.

3. The presence of transverse reinforcement increases the shear transfer capacity of the compression chord due to the vertical confining stresses introduced by the stirrups. As a consequence, the amount of transverse reinforcement needed according to this method is less than in the existing ones.

4. Prestressing effects on the shear strength are taken into account by the model, through the increment of the neutral axis depth and of the cracking moment and through the effects of the prestressing force, inclination and eccentricity on the equilibrium of internal forces.

5. It is considered that, in the positive bending moment zones, the critical crack initiates at the section where the bending moment, at failure, equals the cracking moment. Therefore, the critical crack in PC members is farther from the zero bending moment point than in RC ones

6. Shear-flexure interaction is explicitly accounted for in the model, resulting relevant in those cases where the bending moment at the control section considerably exceeds the cracking moment. This is the case of internal supports of continuous beams or cantilevers, where the bending moments and shear forces increase with the proximity of the support and the critical crack forms near the support.

7. The predictions of the present model fit very well the experimental results of a large data base collected in the new ACI-DAfStb databases of 1287 shear tests on slender reinforced and prestressed concrete beams with and without stirrups. A mean of 1.13 and a CoV of 19,3% and a 5% real percentile of 0.839 are obtained for the proposed method, while a mean of 1.27 a CoV of 35.5 % and a real 5% percentile of 0.804 are obtained for EC2,. This fact indicates that the proposed model is not only less disperse and more precise (and less expensive) but also safer Fthan the current EC2.

8. In the case of beams with T- or I-sections, the contribution of the concrete compression chord may be very important, as opposed to what is considered by most existing codes.

The mechanical character of the model allows extending it in a natural way to punching of slabs, as it has been briefly shown, to other materials (steel fibre reinforced concrete SFRC, FRP reinforced or strengthened concrete beams), to beams strengthened by means of vertical prestressing, to beams s subject to moderate axial loads or to tensile stresses induced by constrained shrinkage and other. Further simplifications are currently being made, after evaluating the relative influence of each parameter, in order to derive simpler equations for practical design, with the minimum loss of accuracy.

The conceptual simplicity, accuracy, adaptability and mechanical character of the model makes it especially adequate for daily engineering practice and for educational purposes.

ACKNOWLEDGEMENTS

REFERENCES

[1] Ferreira, D., Bairán, J., & Marí, A. (2013), Numerical simulation of shear-strengthened RC beams. *Engineering Structures*, *46, 359-374*.

[2] Vecchio, F. J., & Collins, M. P. (1986). The modified compression-field theory for reinforced concrete elements subjected to shear. *ACI J.*, *83(2), 219-231*.

[3] Vecchio, F. (2000). Disturbed stress field model for reinforced concrete: Formulation. *Journal of Structural Engineering*, *126 (9), 1070-1077*.

[4] Bairán, J. & Marí, A. (2006), Coupled model for the nonlinear analysis of anisotropic sections subjected to general 3D loading. Part 1: Theoretical formulation. *Comp. & Str*, *84 (31-32), 2254–2263*.

[5] Bairán, J. & Marí, A. (2007), Multiaxial-coupled analysis of RC cross-sections subjected to combined forces. *Engineering Structures, 29 (8), 1722-38*.

[6] Petrangeli, M., Pinto, P.E., Ciampi, V. (1999), Fiber element for cyclic bending and shear of RC structures. I: Theory. *Journal of Engineering Mechanics, 125 (9), 994-1001*.

[7] Bentz, E.C. (2000), Sectional analysis of reinforced concrete members. Doctoral dissertation, University of Toronto.

[8] Navarro Gregori, J., Miguel, P., Fernández, M.A., Filippou, F.C. (2007). A 3D numerical model for reinforced and prestressed concrete elements subjected to combined axial, bending, shear and torsion loading. *Engineering Structures, 29 (12), 3404-3419.*

[9] Saritas, A. & Filippou, FC. (2009), Inelastic axial-flexure-shear coupling in a mixed formulation beam finite element. *Int J Non Linear Mech, 44 (8), 913-922*.

[10] Mohr, S., Bairán, J.M., Marí., A.R. (2010), A frame element model for the analysis of reinforced concrete structures under shear and bending. *Eng. Struct, 32 (12), 3936-3954*.

[11] Reineck, K. (1991). Ultimate shear force of structural concrete members without transverse reinforcement derived from a mechanical model. *ACI Structural Journal, 88(5), 592-602*.

[12] Zararis, P.D. & Papadakis, G.C. (2001), Diagonal shear failure and size effect in RC beams without web reinforcement. *ASCE J. Struc. Eng., 127 (7), 733-742*.

[13] Choi, K. K., Park, H. G., & Wight, J. K. (2007). Unified shear strength model for reinforced concrete beams - part I: Development. *ACI Structural Journal, 104(2), 142-152.*

[14] Tureyen, A. K., & Frosch, R. J. (2003). Concrete shear strength: Another perspective. *ACI Structural Journal, 100(5), 609-615*.

[15] Muttoni, A., & Ruiz, M. F. (2008). Shear strength of members without transverse reinforcement as function of critical shear crack width. *ACI Structural Journal, 105(2), 163-172*.

A unified mechanical model for design and assessment of concrete structures in shear and punching
Third International Conference on Mechanical Models in Structural Engineering
University of Seville. 24-26 june 2015.

[16] Wolf, T. S., & Frosch, R. J. (2007). Shear design of prestressed concrete: A unified approach. *Journal of Structural Engineering, 133(11), 1512-1519*.

[17] Park, HG, Kang. S; Choi, K. (2013), Analytical model for shear strength of ordinary and prestressed concrete beams, *Engineering Structures 46 (2013) 94–103*

[18] Collins, M. P., Bentz, E. C., Sherwood, E. G., & Xie, L. (2008), An adequate theory for the shear strength of reinforced concrete structures. *Mag. of Conc. Res., 60 (9), pp.635-650*.

[19] Recupero, A., D'Aveni, A., Ghersi, A. (2013), NMV interaction domains for box and I-shaped reinforced concrete members. *ACI Structural Journal, 100 (1), pp. 113-119*.

[20] Canadian Standards Association, CAN/CSA-A23.3-04 (R2010) - Design of Concrete Structures.

[21] Federation Internationale du Béton. Model Codel 2010 for concrete structures. Erhnst and Sohn

[22] ACI Committee 318 (2008), Building Code Requirements for Structural Concrete (ACI 318-08) and Commentary. American Concrete Institute. Farmington Hills, MI, USA.

[23] Eurocode 2 (2002), Design of Concrete Structures: Part 1: General Rules and Rules for Buildings. European Committee for Standardization.

[24] Marí, A., Bairán, J., Cladera., A., Oller, E. & Ribas, C. (2014). Shear-flexural strength mechanical model for the design and assessment of reinforced concrete beams. *Struct & Infrastr. doi: 10.1080/15732479.2014.964735*.

[25] Marí, A., Cladera, A., Barán, A., Oller, E., Ribas, C., 2015). Un modelo de resistencia a flexión y cortante de vigas esbeltas de hormigón armado (2015), *Hormigón y Acero No. 274*.

[26] Cladera A. Marí A, Ribas C.Bairán J, Oller, E. (2015). Predicting the shear-flexural strength of slender reinforced concrete T and I shaped beams. *Engineering structures* (in review)

[27] Reineck, K. H., Bentz, E. C., Fitik, B., Kuchma, D. A. & Bayrak, O. (2013). ACI-DAfStb database of shear tests on slender reinforced concrete beams without stirrups. *ACI Structural Journal, 110(5)*

[28] Reineck, K. H., Bentz, E., Fitik, B., Kuchma, D. A., & Bayrak, O. (2014). ACI-DAfStb Databases for Shear Tests on Slender Reinforced Concrete Beams with Stirrups. *ACI Structural Journal, 111(5)*.

[29] ACI-DAfStb 617 (2015): ACI-DAfStb databases 2015 on shear tests for evaluating relationships for the shear design of structural concrete members without and with stirrups. Report for Research Project DAfStb V479. Reineck, K.-H.; Dunkelberg, D. (Eds.). DAfStb H. 617, Beuth Verl. Berlin.

[30] ASCE-ACI Committee 445 (1998), Recent approaches to shear design of structural concrete. American Concrete Institute.

[31] Kupfer, H. B., & Gerstle, K. H. (1973), Behavior of concrete under biaxial stresses. *Journal of the Engineering Mechanics Division, 99 (4), 853-866*.

[32] Marí, A., Cladera, A., Oller, E., Bairán, J. (2014) Shear design of FRP reinforced concrete beams without transverse reinforcement, *Composites Part B: Engineering, 57, 228-241.*

[33] Oller, E., Marí, A., Bairán, J., Cladera, A. (2015), Shear design of reinforced concrete beams with FRP longitudinal and transverse reinforcement. *Composites Part B: Engineering*, 74, Pp 104-122